Measuring Key Parameters Governing Anion Transport Through Mx-80 Bentonite

Conference or Workshop Item

CSCE 2021 Annual Conference
Inspired by Nature – Inspiré par la Nature

26-29 May 2021

MEASURING KEY PARAMETERS GOVERNING ANION TRANSPORT THROUGH MX-80 BENTONITE

Chowdhury, F.[1,3], Rashwan, T. L.[1], Papry, S. A.[1], Behazin, M.[2], Keech, P. G.[2], Mondal, P.[1], Sharma, J.[1], and Krol, M.[1]
[1] Department of Civil Engineering, Lassonde School of Engineering, York University, Canada
[2] Nuclear Waste Management Organization, Canada
[3] farah215@yorku.ca

Abstract: The Nuclear Waste Management Organization (NWMO) is responsible for the design and implementation of Canada's deep geological repository (DGR), which will be constructed ~500 m below ground surface to safely contain and isolate used nuclear fuel. Used fuel containers (UFC), designed by NWMO as part of multi-barrier system for DGR, comprises of an inner steel core with an outer copper layer that serves as a corrosion barrier. Surrounding the UFC, a highly compacted MX-80 bentonite (HCB) is used to suppress the transport of corrosive agents to the UFC and to limit the movement of radionuclides out of the DGR, in the highly unlikely event of a UFC failure. Under anaerobic conditions, sulfate reducing bacteria at the interface of the host rock and bentonite may produce bisulfide (HS^-) that can transport to the UFC surface and corrode the copper barrier. Therefore, it is crucial to understand HS^- transport mechanisms through bentonite to assess the long-term DGR performance. Due to bentonite's low permeability, HS^- transport will be diffusion-driven; therefore, the apparent diffusion coefficient and retardation are critical parameters for the DGR performance assessment. This study aims to quantify HS^- diffusion through bentonite using diffusion experiments under a range of anticipated DGR conditions (e.g., temperature, ionic concentration). This paper outlines the underpinning theory, experimental methodology developed to conduct experiments, and preliminary results. Altogether, this work bolsters confidence in the experimental design and methodology that will be used to determine necessary key parameters to model reactive transport of HS^- through the DGR's bentonite barrier.

1 INTRODUCTION

Nuclear waste management is a key issue among nuclear energy producing nations. This is a challenging engineering task, as high-level nuclear waste poses a significant risk for hundreds or thousands of years, and an ongoing risk for nearly a million years as the radioactivity dissipates to background levels (Hall et al. 2021). Therefore, nuclear safety agencies around the world agree that deep geological repositories (DGRs) constructed hundreds of meters below ground in stable host rock formations are viable solutions to safely isolate spent nuclear fuel from terrestrial ecosystems (Ewing 2015, Briggs et al. 2017b, Hall et al. 2021). The Nuclear Waste Management Organization (NWMO) is responsible for designing and implementing Canada's DGR. This design requires that the spent fuel be isolated in the DGR within a multi-barrier engineered system, which contains highly compacted MX-80 bentonite that surrounds the copper-coated used fuel containers (UFCs). The compacted bentonite serves many purposes, one of which is to retard the migration of corrosive species to the UFC. Microbially influenced corrosion is one of the key corrosion mechanisms that is currently under investigation by NWMO and other nuclear agencies (Salonen et al. 2021). That is, sulfate-reducing bacteria at the interface of the bentonite and host rock may produce bisulfide (HS^-) if a sufficient supply of sulfate is present (Briggs et al. 2017b, Hall et al. 2021). This HS^- may

then transport through the bentonite and corrode the copper coating of the UFC, and potentially compromise the integrity of the containment system. Therefore, it is critical to understand the parameters that govern HS^- transport through bentonite under the anticipated DGR conditions. As shown by recent modelling work, since the diffusive-driven transport of HS^- from the outer rock limits the extent of corrosion, these parameters need to be well-resolved across the conditions expected in the DGR (Briggs et al. 2017a, Briggs et al. 2017b).

This project aims to provide direct measurements of these HS^- transport parameters under the range of conditions expected in the Canadian DGR (e.g., temperature, ionic concentrations, pH). However, because compacted MX-80 bentonite (which has a complex structure and swelling behaviour) and HS^- (which as high reactivity) are challenging materials to experiment with, extensive preliminary work has been completed to develop robust experimental infrastructure and methodologies. Chloride (Cl^-) diffusion experiments were conducted to benchmark against other diffusion experiments in the literature and confirm the experimental setup and methodology are appropriate for measuring HS^- transport through bentonite. Preliminary HS^- sorption experiments were also performed. This paper outlines the underpinning theory, experimental methodology, and preliminary results developed to conduct these experiments. Altogether, the objective of this work is to build confidence in the experimental methodology and design that will aid in validation of reactive-transport models of HS^- through bentonite in a DGR.

2 METHODOLOGY

2.1 Diffusion Experiments

2.1.1 Mathematical Description of Diffusion Experiments

Through-diffusion experiments are commonly used to measure the diffusivity of a species through bentonite (García-Gutiérrez et al. 2006, Van Loon et al. 2007, Shackelford and Moore 2013). These experiments are conducted using varying concentrations on both sides of a diffusion cell, which are kept relatively constant throughout an experiment (see Figure 1). By assuming that Fick's second law describes diffusion-driven transport, and considering sorption, the governing transport equation is:

$$[1] \quad \phi \frac{\partial C}{\partial t} = \phi D_p \frac{\partial^2 C}{\partial x^2} - \rho_d \frac{\partial C_s}{\partial t}$$

where, ϕ is the porosity, ρ_d is the dry density, $D_e = \phi D_p$ is the effective diffusion coefficient – where the pore diffusion coefficient, D_p, accounts for the pore structure lengthening the diffusion length, e.g., due to tortuosity (Shen and Chen 2007). Moreover, these three coefficients are assumed to be constant in time and space. If sorption can be described using a linear isotherm, $C_s = K_d C$, to relate the species concentration in the solid and aqueous phases (C_s and C, respectively) using a constant equilibrium coefficient, K_d, then Equation 1 can be simplified as:

$$[2] \quad \frac{\partial C}{\partial t} = D_a \frac{\partial^2 C}{\partial x^2}$$

where the apparent diffusion coefficient, $D_a = D_e/(\phi + \rho_d K_d)$, accounts for the retardation due to sorption. While the formulation of Equation 2 is widely used to analyze diffusion experiments in bentonite, the actual diffusive process may be complicated by numerous factors including: (*i*) the system's geochemistry, (*ii*) the influence of surface or interlayer diffusion between clay particles (thereby necessitating that the solid phase be modelled to rigorously capture the true transport physics), and (*iii*) the possibility of a semipermeable membrane behaviour because of anion exclusion (anion exclusion describes how anions can only pass through narrow fractions of the pore space in bentonite because the negative charge from the surface of the clay particles repels the anions) (Van Loon et al. 2007, Shackelford and Moore 2013). Though these effects are not explicitly modelled in the idealized formulations in Equations 1 and 2, they are worth considering in interpreting reactive anion transport through bentonite, such as HS^-.

The boundary conditions of a through-diffusion experiment are described as:

[3] $C(x > 0, t = 0) = 0\,; C(x = 0, t > 0) = C_0\,; C\left(x = x_f, t > 0\right) = 0;$

which assumes the bentonite thickness is x_f, the bentonite is initially free of the species, and the in- and out-reservoir species concentrations are constant with time at C_0 and 0, respectively. These boundary conditions are practically maintained by using: (*i*) a large (> 1 L) in-reservoir (at $x = 0$, so that the changes in the inflow concentration due to diffusive transport does not vary by more than 5%) and (*ii*) a small (< 0.02 L) out-reservoir (at $x = x_f$), which is replaced frequently so that the concentration contains measurable amount of the species, but less than 10% of the in-reservoir concentration (García-Gutiérrez et al. 2006, Van Loon et al. 2007).

With these boundary and initial conditions, an analytical solution to Equation 2 can be obtained (Crank 1979):

[4] $$\frac{C}{C_0} = 1 - \frac{x}{x_f} - \frac{2}{\pi}\sum_{n=1}^{\infty}\frac{1}{n}\sin\left(\frac{n\pi x}{x_f}\right)\exp\left(-\frac{n^2\pi^2 D_a t}{x_f^2}\right)$$

By integrating Equation 3 throughout time, the total mass (M) of the species passing through the bentonite system can be described as:

[5] $$M = C_0 x_f A(\phi + \rho_d K_d)\left[\frac{D_a t}{x_f^2} - \frac{1}{6} - \frac{2}{\pi^2}\sum_{n=1}^{\infty}\frac{(-1)^n}{n^2}\exp\left(-\frac{n^2\pi^2 D_a t}{x_f^2}\right)\right]$$

At late times, the series expansion in Equation [5] trends to zero and an approximate solution emerges as:

[6] $$M = C_0 A\left[\frac{D_e t}{x_f} - \frac{(\phi + \rho_d K_d)x_f}{6}\right]$$

Equation 6 greatly simplifies the full problem and provides a straightforward tool to extract useful information from through-diffusion experiments. That is, by fitting the late-time data using a simple linear regression, through-diffusion experimental data can provide a direct measurement of D_e. Moreover, when using a conservative anion, Equation 6 can also provide insight into the *diffusion-accessible porosity*. Due to the anion exclusion effect in bentonite (described above), anions are not able to transport through the entire pore space. Therefore, the ϕ measured from through-diffusion experiments using a conservative anion, such as chloride (Cl^-), is often much lower than the full pore space (Van Loon et al. 2007). In addition, Equation 6 shows how the influence of sorption (and perhaps other geochemical reactions encompassed in the term) manifest in analyzing through-diffusion experiments. However, because there are two phenomena that may affect diffusive transport (i.e., the anion exclusion effect and sorption/geochemical reactions), it is best to investigate the influence sorption/geochemical reactions in independent batch experiments, as these phenomena are not easily untangled from the results from through-diffusion experiments.

2.1.2 Equipment Description of Diffusion Experiments

The experimental setup in this study followed best practices established by others for investigating species transport in bentonite via through-diffusion experiments (García-Gutiérrez et al. 2006, Van Loon et al. 2007, Bengtsson and Pedersen 2016, Pedersen et al. 2017). Figure 1 illustrates a schematic of the experimental setup. Custom-made diffusion cells were fabricated using 316L stainless steel (SS) to provide good durability against the large pressures produced from bentonite swelling (1-10 MPa) (Dixon et al. 2018), and sufficient resistance against HS^- corrosion. Within the diffusion cell, 5 mm thick MX-80 bentonite pucks (25 mm diameter) were placed in between polytetrafluoroethylene (PTFE) membranes (25 mm diameter and pore size 0.1 µm) and porous 316L SS discs (shaved to 25 mm diameter, 1.6 mm thick, pore diameter 10 µm, 9446T34, McMaster Carr). The SS porous discs were washed with soap water, 30% methanol, and

5% nitric acid to remove impurities from the fabrication process, and then saturated with DI water in a Pyrex vacuum desiccator. All fittings used were also made of 316L SS and washed prior to experimentation. As shown in Figure 1, only SS, PTFE, and Norprene tubing were used throughout the system, and all tubing was flushed with 5% nitric acid prior to experimentation. A peristaltic pump (0.01-100 rpm, HV-07522-30, Masterflex) was used to circulate solution in the in- and out-reservoirs to maintain the boundary conditions described in Equation 3. At the base of the diffusion cell, a compression button load cell (0-200 kg, CZL204E, Phidgets Inc.) measured swelling pressure throughout the saturation process. All MX-80 bentonite samples were provided by NWMO at an initial dry density and moisture content of 1800 kg m^{-3}, and 17%, respectively. A detailed review of MX-80 bentonite properties was recently provided by Dixon et al. (2018). Once placed within the cell, the bentonite pucks were saturated with DI water (thereby causing swelling), and then exposed to a concentration gradient between the in- and out-reservoirs, which drove diffusion.

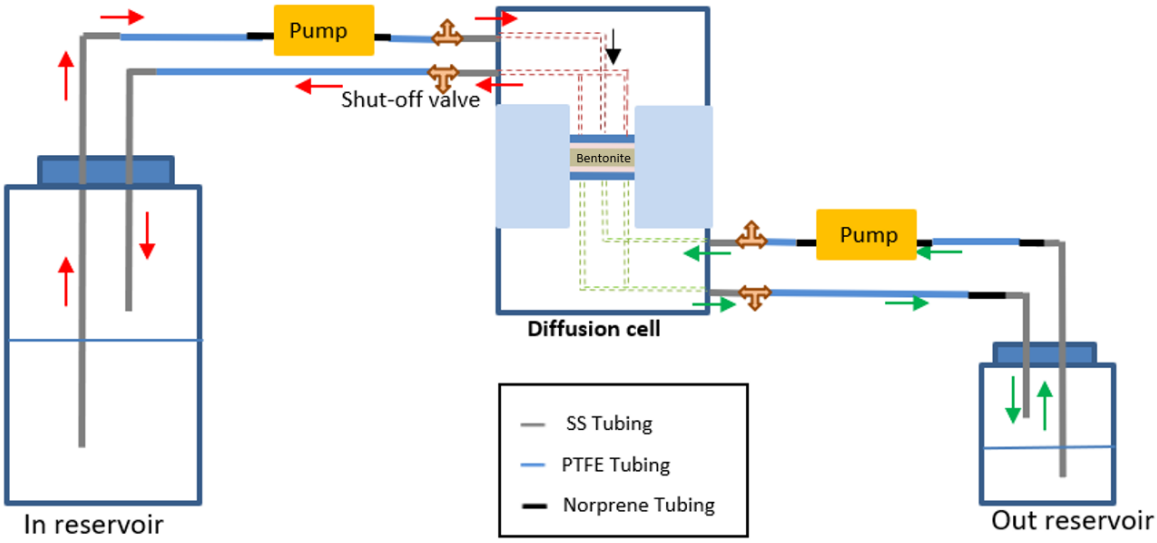

Figure 1: Schematic of the through-diffusion experimental layout.

2.2 Batch Sorption Experiments

Batch experiments allow for better understanding of the role of sorption phenomena (and geochemical reactions) in HS^- transport. Preliminary batch sorption experiments were performed following best practices in the literature, e.g., (Alinnor 2007, Xu et al. 2008, Gupt et al. 2019), and used granulated MX-80 bentonite (obtained from NWMO). These experiments explored the effects of contact time (1 and 24 hours) and liquid:solid mass ratios (L:S, 50, 100, and 200) on sorption behaviour. The other experimental conditions were kept constant such as: HS^- initial concentrations (0.9 mg L^{-1}), pH (9), and ambient laboratory temperatures. Prior to the experiments, HS^- stock solutions were prepared by dissolving sodium sulfide nonahydrate ($Na_2S{\cdot}9H_2O$) in deoxygenated water (prepared by purging nitrogen gas) following the standard method 4500-S2-A. Bentonite stock solutions were prepared by mixing dried bentonite powder in deoxygenated water at L:S = 20 and sonicated with a bath sonicator (VWR Symphony 97043-936 Ultrasonic Cleaner) to ensure the bentonite was well dispersed. Sample solutions were prepared in 50 mL Pyrex glass centrifuge tubes (Fisher Scientific) by mixing required amount of bentonite and HS^- stock solutions and diluting with deoxygenated water to obtain the desired L:S and HS^- concentration. The pH values were adjusted by using 0.1 M NaOH. For each set of samples, two different types of experimental blanks were prepared: (*i*) with bentonite but no HS^- and (*ii*) with HS^- but no bentonite. Type (*i*) was used to indicate the background absorbance (i.e., the combined effect of particle interference and presence of background HS^-) and type (*ii*) was used to monitor the loss of HS^- due to experimental effects other than sorption. All the samples and blanks were prepared in an anaerobic chamber to best simulate the anoxic conditions expected in a DGR and to minimize HS^- oxidation. After sample preparation, the centrifuge tubes were

shaken using a tube rotator (MX-RD-Pro, SCILOGEX) at 60 rpm for 1 or 24 hours. After mixing, the solid and liquid phases were separated by centrifuging the solutions at 3500 rpm for 1 hour and subsequently stage-filtrated with 1, 0.45, and 0.2 µm syringe filters (Fisher Scientific). Finally, the equilibrium HS^- concentration in the liquid phase was measured using the methylene blue method (standard methods, SM 4500-S2 D) with a spectrophotometer (Hach DR 6000, Hach) at a wavelength of 665 nm. This method was chosen as it is a simple, inexpensive method that has a sufficiently low detection limit for HS^- (estimated here as 0.02 mg L^{-1}) (Pedersen et al. 2017). A calibration curve for the methylene blue method is presented in Figure 2.

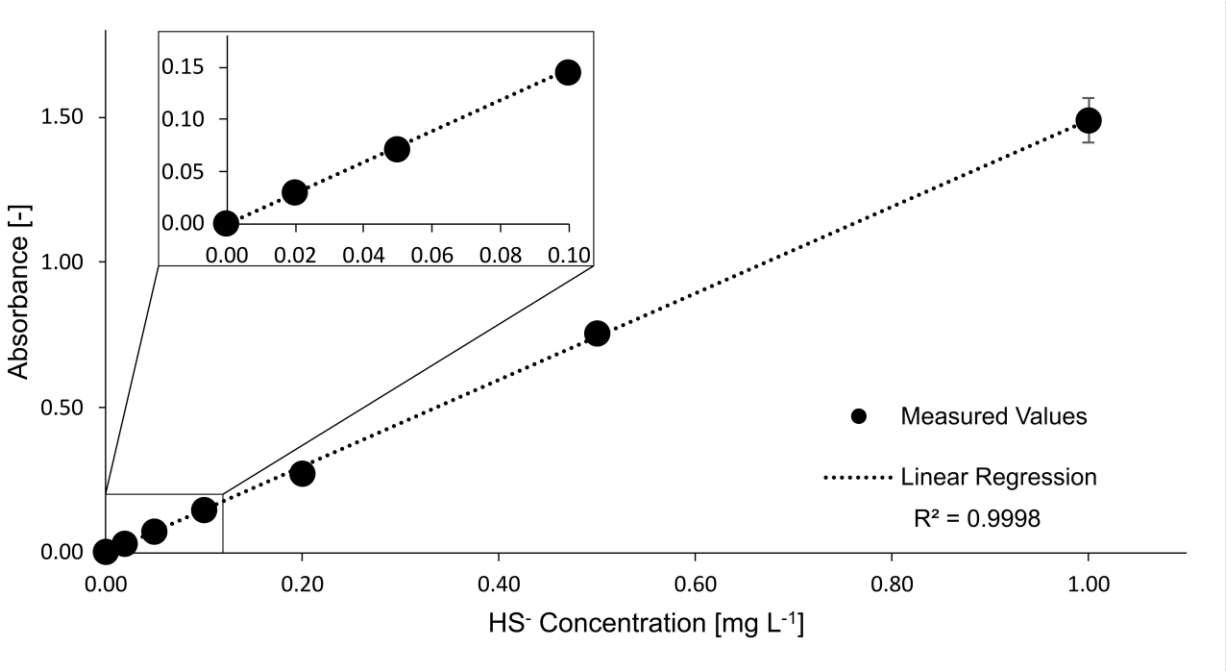

Figure 2: Calibration plot for measuring HS^- concentration using the methylene blue method for HS^- concentration ranging over 0 to 1 mg L^{-1}. The linear line of best fit (forced to a y-intercept = 0) and coefficient of determination (R^2) indicate good confidence in the calibration procedure. The inset highlights the good reliability at low HS^- concentrations (< 0.1 mg L^{-1}). Note that all data points represent the average of two repeat measurements, where the error bars represent the maximum and minimum measurements (which are not visible on most data points due to the small error).

From the measured equilibrium HS^- concentration, the sorption efficiency and sorption capacity were calculated following Equations 7 and 8:

[7] $$Sorption\ Efficiency = \left(\frac{C_i - C_e}{C_i}\right) \times 100\%$$

[8] $$Sorption\ Capacity = (C_i - C_e)\left(\frac{V}{m}\right)$$

Where C_i is the initial HS^- solution concentration (with concentration from blank (*ii*) subtracted to account for the experimental effects after shaking for 1 or 24 hours), C_e is the HS^- solution concentration at equilibrium after shaking for 1 or 24 hours (with concentration from blank (*i*) subtracted to account for the interference from small bentonite particulates and background HS^-), V is the solution volume, and m is the bentonite mass.

2.3 Cl^- Diffusion Experiments

A Cl^- diffusion experiment was first performed to test the reliability and performance of the experimental setup and methodology. Cl^- is a common, conservative anion tracer that is widely used in bentonite through-diffusion experiments (Van Loon et al. 2003, García-Gutiérrez et al. 2006, Van Loon et al. 2007, Shackelford and Moore 2013). To test Cl^- diffusion, a solution of 1 M Cl^- was prepared by mixing reagent-grade NaCl within de-ionized (DI) water. The Cl^- concentration was then measured in the out-reservoir (which was regularly replaced with fresh DI water to maintain the zero-concentration boundary condition detailed in Equation 3) using ion chromatography (Thermo Scientific™ Dionex Ion Chromatograph).

3 RESULTS AND DISCUSSION

3.1 Swelling Pressure Results

Figure 3 presents the swelling pressure results measured from the load cell over time as the bentonite sample became saturated with DI water while the in-reservoir pump was circulated, and the out-reservoir tubing was left open to allow the air to escape. This swelling history illustrates the characteristic swelling behaviour of bentonite expected during saturation, as the maximum swelling of 2.7 MPa in Figure 3 was reached soon after 5 days (Van Loon et al. 2007, Villar et al. 2010). The maximum swelling values were confirmed after approximately 5 months, as this swelling experiment was performed for an unusually long time during the closures from the first COVID-19 provincial lockdown from March to August 2020. The spike in swelling pressure up to 2.9 MPa after 174 days corresponded to when the DI water in the out-reservoir was connected to allow saturation from the top, which was also expected and seen by others (Van Loon et al. 2007). Altogether, Figure 3 illustrates that the characteristic bentonite swelling behaviour with time was well-captured in the experimental setup.

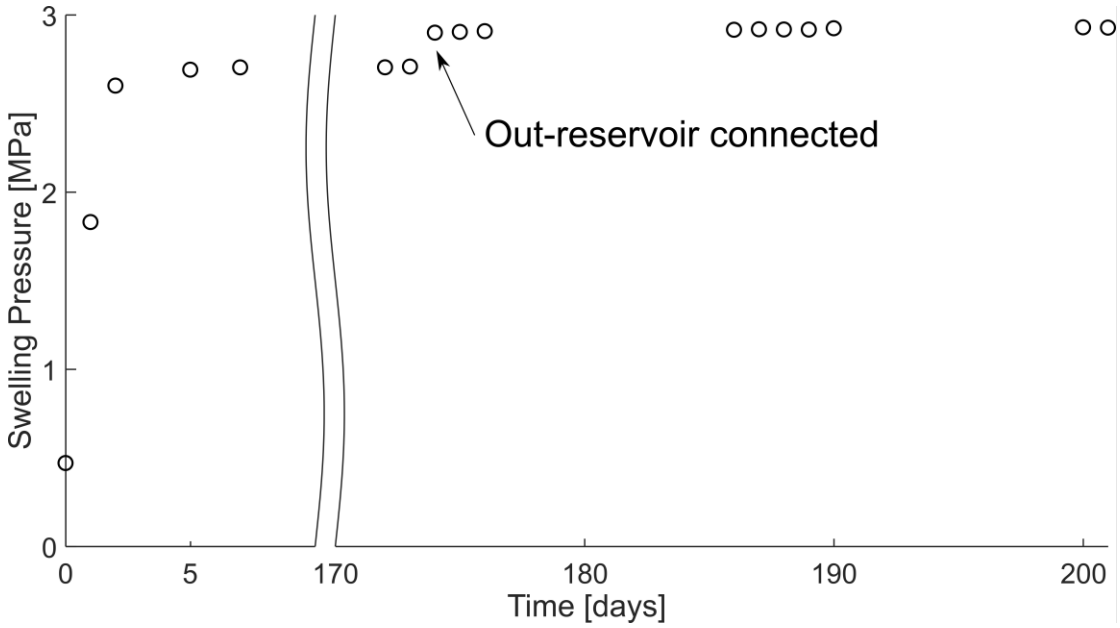

Figure 3: Swelling pressure measured during saturation with DI water, and the spike in swelling pressure at 174 days coincided with connecting the out-reservoir to DI water to allow saturation from the top of the cell.

3.2 Cl^- Diffusion Results

Figure 4 presents the results from the Cl^- diffusion experiment over time and the modelled behaviour using Equation 5 (further described below). This figure shows the cumulative Cl^- mass that diffused throughout the bentonite sample from the in-reservoir and was measured in the out-reservoir. Similar to the

characteristic swelling behaviour seen in Figure 3, Figure 4 shows the characteristic diffusion behaviour expected during Cl^- diffusion. As shown in the inset in Figure 4, an approximate linear profile was established relatively quickly after the first day of experimentation, and the following diffusion was well characterized using the approximate solution in Equation 6. Therefore, because Cl^- is a non-sorbing tracer (i.e., $K_d \approx 0$), both the diffusion-accessible porosity and effective diffusivity were estimated from performing a linear regression on the experimental results. This analysis calculated an effective diffusivity $(D_e) = 1 \times 10^{-11}$ m^2 s^{-1} and a diffusion-accessible porosity (ϕ) = 0.043. Note that the actual porosity in this sample was close 0.30-0.40, implying that only ~10% of the pore space was accessible to diffusion. Figure 4 illustrates that the characteristic diffusion behaviour was well-captured following the experimental methodology.

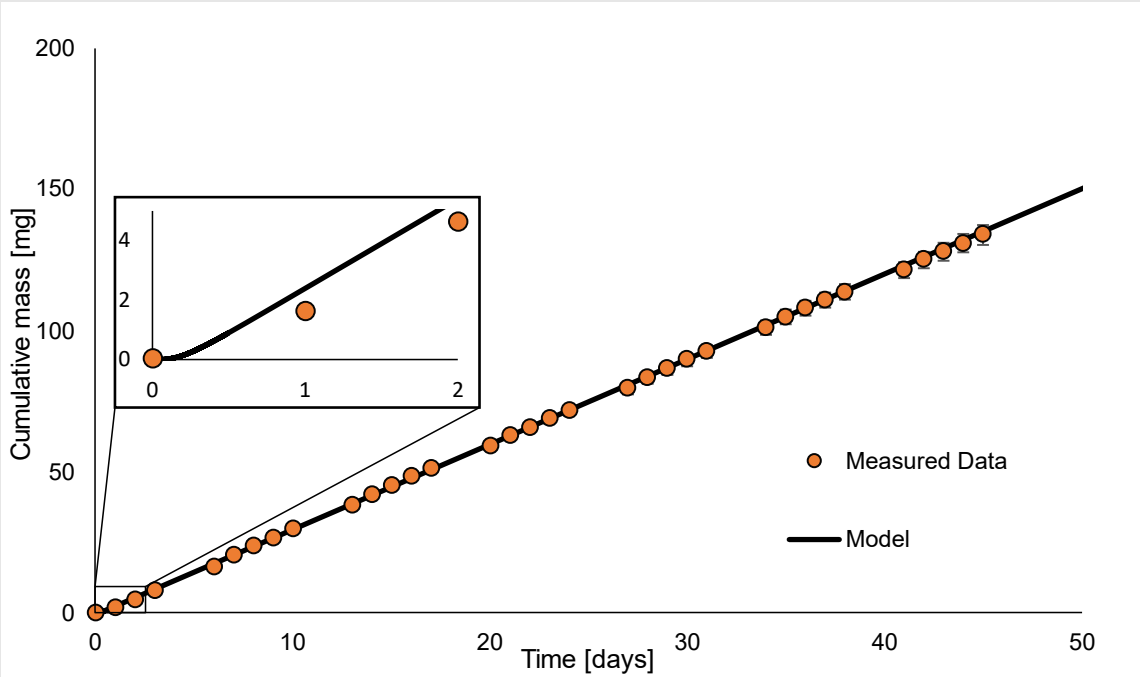

Figure 4: The cumulative Cl^- mass measured during a through-diffusion experiment, where the orange circles note the experimental measurements, and the solid line represents the modelled behaviour using Equation 5. The inset shows only the first two days to highlight that the infinite expansion in Equation 5 trends to zero after ~0.5 days of diffusion. Note that all data represents the average of 2 to 4 repeat measurements, where the error bars represent the 99.9% confidence interval of measurements (which are not visible on most data points due to the small error).

3.2.1 Discussion on Swelling Pressure and Cl^- Diffusion

As this experimental methodology and infrastructure are newly established, it is important to compare the swelling pressure (Figure 3) and Cl^- diffusion (Figure 4) results with published data. First, the swelling data from this experiment (2.9 MPa) using DI water and MX-80 bentonite with an initial dry density of 1800 kg m^{-3} seems unusually low. Other researchers, e.g., (Karnland et al. 2005, Karnland et al. 2006, Navarro et al. 2017, Dixon et al. 2018), suggest that MX-80 bentonite with an initial dry density of 1800 kg m^{-3} should exhibit a much higher swelling pressure (> 10 MPa). Conversely, the Cl^- D_e appears to be higher than reported by others. For example, Van Loon et al. (2007) found from a similar clay at a dry density of 1600 kg m^{-3} had a Cl^- D_e between 4×10^{-13} to 1×10^{-11} m^2 s^{-1} and at a dry density of 1900 kg m^{-3} had a Cl^- D_e between 3×10^{-14} to 1×10^{-12} m^2 s^{-1}. The range of D_e values measured by Van Loon et al. (2007) was due to varying the ionic strength (and thereby the influence of the anion exclusion effect), where 0.01 M and 1 M concentrations of NaCl coincided with the low and high D_e values, respectively.

Though it is difficult to clearly identify the source of the discrepancy here, mainly because of the heterogeneous nature of MX-80 bentonite and the sparse experimental data gathered so far, these two data sources suggest that the bentonite density was lower than expected. That is, by comparing with literature on the swelling pressure and Cl^- D_e, it appears that effective sample dry density may have been closer to 1500 kg m^{-3}, rather than 1800 kg m^{-3}. This discrepancy is expected to have been caused as the bentonite expanded slightly in the sample holder and thereby lowered the density. Because a relatively small sample volume was used in this experiment (only 5 mm thick and 25 mm in diameter), small volume changes (e.g., 1 mm increase in sample thickness) could have had a large impact on the sample density. Therefore, it is important to extract multiple sources of data from these experiments to have a more information to troubleshoot and understand the influence of the experimental setup (e.g., as done here with the swelling pressure and diffusive transport measurements). In addition, though these experiments are still ongoing, the final wet density will be measured when the experiments are complete. This final density measurement will help confirm or refute this hypothesis on how the sample's density may have affected these results and inform best practices for future experiments.

3.3 HS^- Sorption Results

Figure 5 presents the key results from the preliminary sorption experiments testing the effect of L:S and contact time on HS^- sorption. As expected, Figure 5(a) shows that the sorption efficiency was very high at low L:S values (96-99% at 50 L:S) and decreased as the L:S value increased (57-66% at 200 L:S). In other words, as the solids percentage decreased (compared to liquid), the sorption capacity decreased. Similarly, the sorption capacity increased over this same L:S range (shown in Figure 5(b)), i.e., 33-34 to 79-90 mg_{HS} $g^{-1}_{bentonite}$ at 50 to 200 L:S, respectively. These two results reflect how higher L:S ratios have less soil mass and therefore less sorption sites. Furthermore, Figures 5(a) and 5(b) also show that the experiments using either 1- or 24-hour contact times exhibited very similar sorption behaviour. This result suggests that most of the sorption of HS^- occurred within the first hour of contact with bentonite.

These preliminary results compare well with the hypotheses from Pedersen et al. (2017), who suggested that a large fraction of HS^- will likely immobilize in bentonite due to reacting with the ferric and ferrous ions in the MX-80 bentonite. Therefore, these sorption results likely encompass geochemical interactions as well as adsorption. Although the role of geochemical reactions is not yet understood from these preliminary experiments, the initial data suggests that the immobilization of HS^- in bentonite is a significant and rapid process that will inhibit HS^- transport in bentonite.

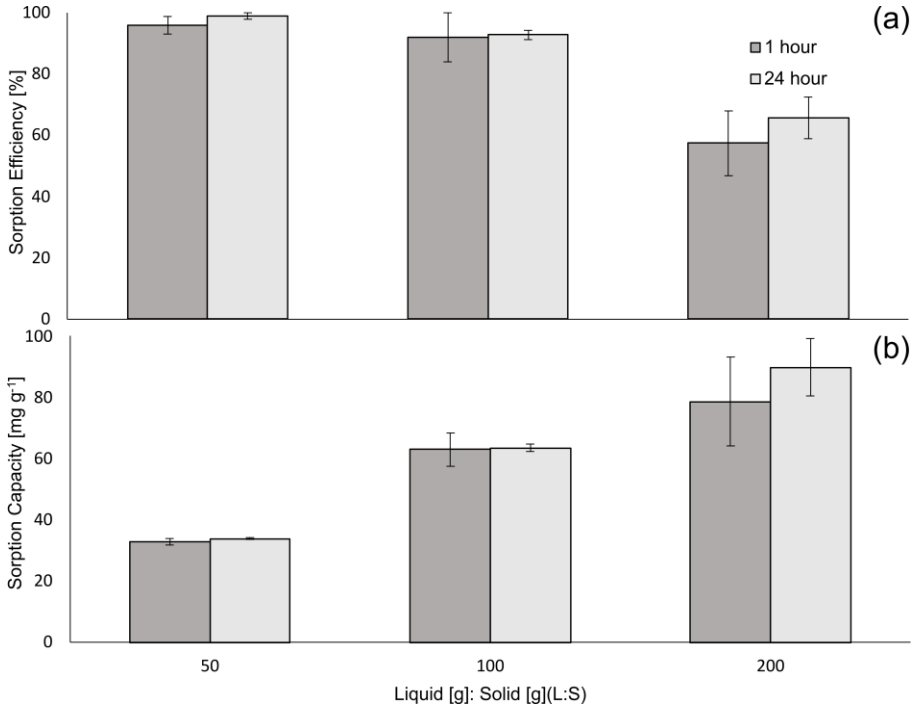

Figure 5. The effect of L:S and contact time on the (a) sorption efficiency and (b) sorption capacity of HS^- on MX-80 bentonite. All data bars represent an average of duplicate experiments and the error bars note the maximum and minimum measurements from duplicate experiments.

4 CONCLUSION

The preliminary results illustrate that the newly developed experimental setup and methodologies capture characteristic diffusion and swelling pressure data as a function of time. However, compared to others in the literature, the maximum swelling pressure and effective Cl^- diffusion coefficient appear to be unusually low and high, respectively. These discrepancies are hypothesized to have resulted from bentonite expansion. However, this effect can be corrected for by measuring the final bentonite density when the sample is extruded after experimentation. In addition, these results underscore the value in pairing swelling pressure measurements with the concentration measurements in a through-diffusion experiment with bentonite, as they can be used to troubleshoot the experimental methodology and correct for experimental effects. The preliminary HS^- sorption results also show expected trends, but further experimentation is needed to understand the fundamental reasons that govern the apparent sorption behaviour (i.e., the role of geochemical reactions).

5 ACKNOWLEDGEMENTS

Funding was provided by the Ontario Research Fund – Research Excellence grant and the Natural Sciences and Engineering Research Council of Canada Collaborative Research and Development Grant in partnership with the Nuclear Waste Management Organization (Toronto, Canada).

6 REFERENCES

Bengtsson, A. and Pedersen, K. 2016. Microbial sulphate-reducing activity over load pressure and density in water saturated Boom Clay. *Applied Clay Science*, **132-133**, 542-551.

Briggs, S., McKelvie, J., Keech, P., Sleep, B. and Krol, M. 2017a. Transient modelling of sulphide diffusion under conditions typical of a deep geological repository. *Corrosion Engineering, Science and Technology*, **52**(sup1), 200-203.

Briggs, S., McKelvie, J., Sleep, B. and Krol, M. 2017b. Multi-dimensional transport modelling of corrosive agents through a bentonite buffer in a Canadian deep geological repository. *Science of the Total Environment*, **599-600**, 348-354.

Crank, J. 1979. *The mathematics of diffusion*, Oxford university press

Dixon, D. A., Man, A., Rimal, S., Stone, J. and Siemens, G. 2018. Bentonite Seal Properties in Saline Water. Toronto, Ontario, Nuclear Waste Management Organization. **NWMO TR-2018-20**.

Ewing, R. C. 2015. Long-term storage of spent nuclear fuel. *Nature Materials*, **14**(3), 252-257.

García-Gutiérrez, M., Cormenzana, J., Missana, T., Mingarro, M. and Molinero, J. 2006. Overview of laboratory methods employed for obtaining diffusion coefficients in FEBEX compacted bentonite. *Journal of Iberian Geology*, **32**(1), 37-53.

Hall, D. S., Behazin, M., Jeffrey Binns, W. and Keech, P. G. 2021. An evaluation of corrosion processes affecting copper-coated nuclear waste containers in a deep geological repository. *Progress in Materials Science*, **118**, 100766.

Karnland, O., Muurinen, A. and Karlsson, F. 2005. Bentonite swelling pressure in NaCl solutions–Experimentally determined data and model calculations. Advances in Understanding Engineered Clay Barriers: Proceedings of the International Symposium on Large Scale Field Tests in Granite, Sitges, Barcelona, Spain, 12-14 November 2003. E. E. Alonso and A. Ledesma, CRC Press**:** 241-256.

Karnland, O., Olsson, S. and Nilsson, U. 2006. Mineralogy and sealing properties of various bentonites and smectite-rich clay materials. Svensk Kärnbränslehantering AB, Swedish Nuclear Fuel and Waste Management Co. **SKB-TR-06-30**.

Navarro, V., De la Morena, G., Yustres, Á., González-Arteaga, J. and Asensio, L. 2017. Predicting the swelling pressure of MX-80 bentonite. *Applied Clay Science*, **149**, 51-58.

Pedersen, K., Bengtsson, A., Blom, A., Johansson, L. and Taborowski, T. 2017. Mobility and reactivity of sulphide in bentonite clays – Implications for engineered bentonite barriers in geological repositories for radioactive wastes. *Applied Clay Science*, **146**, 495-502.

Salonen, T., Lamminmäki, T., King, F. and Pastina, B. 2021. Status report of the Finnish spent fuel geologic repository programme and ongoing corrosion studies. *Materials and Corrosion*, **72**(1-2), 14-24.

Shackelford, C. D. and Moore, S. M. 2013. Fickian diffusion of radionuclides for engineered containment barriers: Diffusion coefficients, porosities, and complicating issues. *Engineering Geology*, **152**(1), 133-147.

Shen, L. and Chen, Z. 2007. Critical review of the impact of tortuosity on diffusion. *Chemical Engineering Science*, **62**(14), 3748-3755.

Van Loon, L. R., Glaus, M. A. and Müller, W. 2007. Anion exclusion effects in compacted bentonites: Towards a better understanding of anion diffusion. *Applied Geochemistry*, **22**(11), 2536-2552.

Van Loon, L. R., Soler, J. M. and Bradbury, M. H. 2003. Diffusion of HTO, 36Cl− and 125I− in Opalinus Clay samples from Mont Terri: Effect of confining pressure. *Journal of Contaminant Hydrology*, **61**(1), 73-83.

Villar, M. V., Gómez-Espina, R. and Lloret, A. 2010. Experimental investigation into temperature effect on hydro-mechanical behaviours of bentonite. *Journal of Rock Mechanics and Geotechnical Engineering*, **2**(1), 71-78.